JCTC Journal of Chemical Theory and Computation

Article

pubs.acs.org/JCTC

Theoretical Study of the Cytochrome P450 Mediated Metabolism of Phosphorodithioate Pesticides

Patrik Rydberg*

Department of Drug Design and Pharmacology, Faculty of Health and Medical Sciences, University of Copenhagen, Universitetsparken 2, DK-2100 Copenhagen, Denmark

Supporting Information

ABSTRACT: The toxicity of phosphorodithioate pesticides is due to the formation of the active oxane product through desulfurization by cytochrome P450 enzymes, both in humans and insects. During this desulfurization, inhibition of cytochrome P450 and a loss of heme has been observed. Here, we study the mechanism of desulfurization and inhibition with density functional theory, using the B3LYP functional with and without dispersion correction. The results show that a reaction mechanism initiated by sulfur oxidation is most likely, with a reaction barrier of 47 kJ/mol. The sulfur oxidation is followed by a ring-closing mechanism with a barrier of 28 kJ/mol relative to the sulfur-oxidized intermediate. The enzymatic contribution to the ring-closing is very small. It is also shown that the apparent loss of heme might be due to the formation of a previously unknown inhibition complex, which changes the aromatic conjugation of the porphyrin ring. We also show that including dispersion correction has significant effects on a ring closure transition state (~30 kJ/mol), whereas effects on the other steps in the reaction are relatively small (4−15 kJ/mol).

INTRODUCTION

The cytochromes P450 (CYPs) are a ubiquitous enzyme family which is involved in the oxidation of a wide range of xenobiotic compounds such as drugs, steroids, vitamins, and pesticides.

Phosphorothioate compounds are used as pesticides in both agricultural and domestic settings. Among the pesticides used today, they are one of the most frequently used compound groups,[1] including compounds such as malathion, parathion, and phorate (see Figure 1). Significant exposure to these chemicals can in mammals result in cholinergic crisis due to phosphorylation and the accompanying inhibition of acetylcholinesterase.[2] The inhibition is caused by the oxone form of the phosphorothioates, which is formed through desulfurization by CYPs.

The mechanism of the formation of the oxone complex was studied by Ptashne et al. using radioactively labeled O_2 and H_2O.[3] They determined that the oxygen atom in the oxone originates from O_2, which shows that this oxygen is the one bound to the heme iron atom in the CYPs. They also suggested a reaction mechanism which involves the formation of an intermediate phosphooxathiirane, which in turn rearranges into the oxone and atomic sulfur. However, they could not determine whether the reaction is initiated by the formation of a sulfur−oxygen bond, which then would cyclize to the phosphooxathiirane, or if the oxygen attacks the phosphor−sulfur bond leading to the immediate formation of the phosphooxathiirane. A later study suggested that, on the basis of the likely reaction mechanisms for the formation of byproduct, initiation by an attack on one of the sulfur's lone pairs is the most likely mechanism for the formation of the oxone (mechanism shown in Figure 2).[4]

Multiple studies have shown that bioactivation of phosphorodithioates leads not only to the formation of the phosphorooxone but also to inactivation of the CYPs that are involved in the activation. Coupled to this inactivation is also the decrease of CYPs detectable as their carbon monoxide complexes.[5] The inactivation has shown to at least partly be due to the binding of the sulfur atom (released during the formation of the oxone) to the CYPs. The binding of sulfur atoms to the protein seems to be almost exclusive to the CYPs; binding to other proteins has not been observed. It has also been shown that 50% of the sulfur bound is released as SCN^- when the CYPs are treated with CN^-, indicating the presence of hydrodisulfide linkages, which most likely are formed by the formation of bonds between the released sulfur and cysteine residues in the active site.[6] However, the binding of sulfur to cysteine amino acids in the protein does not explain the decrease of heme content observed in experiments. Halpert et al. hypothesized that this could be because binding of the reactive sulfur atom to the heme iron atom would make the heme iron atom dissociate from the porphyrin moiety, which in turn would make all spectroscopic measurements show the disappearance of heme.[5]

In this work, we study the mechanism of the oxone formation for a model system using density functional theory, in a vacuum and in solvent, and with and without empirical dispersion correction. We also propose a structure for a possible inhibition complex that could explain the apparent disappearance of heme.

COMPUTATIONAL METHODOLOGY

All calculations were performed with the Turbomole software package,[7] version 6.3.1. In the calculations, compound I in the CYPs is modeled by a reduced heme model without side chains, iron porphine with SCH_3^- and O^{2-} as axial ligands.

Received: May 2, 2012

   dx.doi.org/10.1021/ct300347z | J. Chem. Theory Comput. XXXX, XXX, XXX−XXX

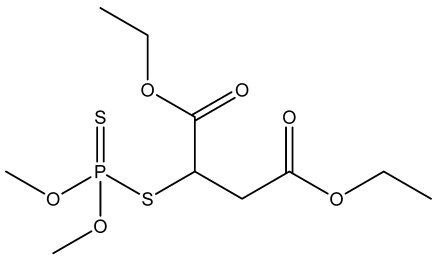

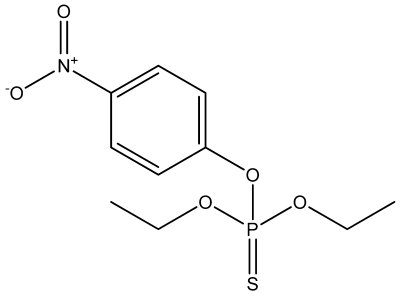

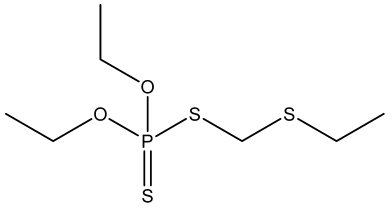

Figure 1. Chemical structures for parathion, malathion, and phorate.

All calculations were performed using the B3LYP functional[8−10] with the VWN(V) correlation functional[11] (unrestricted formalism for open shell systems). The geometry optimizations, frequency calculations, and solvent calculations were performed with the double-ζ basis set of Schäfer et al.,[12] enhanced with a p function with the exponent 0.134915, on the iron atom, and the 6-31G(d) basis set[13−15] for the other atoms. The final energies were determined by single point calculations using the 6-311++G(2d,2p) basis set[16,17] for all atoms, except iron, for which we used the double-ζ basis set of Schäfer et al.,[12] enhanced with s, p, d, and f functions (exponents of 0.01377232, 0.041843, 0.1244, 2.5, and 0.8; two f functions).[18] All transition states were verified to have only one imaginary frequency. The normal modes of the transition states were verified to connect the reactants and products. Charge and spin populations were computed using Mulliken population analysis[19] of the final energy calculations.

Dispersion correction was calculated using the D3 formalism.[20] When calculating dispersion corrected energies, the D3 formalism was used for all calculations (geometry optimizations, frequency calculations, and single point energy calculations).

Solvent calculations were carried out with the continuum conductor-like screening model (COSMO),[21] using an effective dielectric constant (ε) of 4 (except where otherwise mentioned). For the atomic radii, we used the optimized COSMO radii in Turbomole[7] (and 2.0 Å and 1.75 Å, for Fe and P, respectively).

Frequency calculations and solvent calculations were carried out using the smaller basis set combination.

Energies presented in the paper are from the single point calculations with the large basis set, with additional zero-point energy corrections and solvation correction (ε = 4), unless otherwise mentioned. All energies are presented in the Supporting Information.

UV spectra were computed using the ZINDO/S method[22,23] in the ORCA program package, version 2.8.[24]

RESULTS AND DISCUSSION

Enzymatic Formation of the Phosphooxathiirane. In the reactant state (**R**), the ligand was found to coordinate with two methyl groups toward the iron-oxo oxygen atom (Figures 3 and 4). The distance between the methyl hydrogen atoms and the oxygen atom was shortened by almost 0.2 Å when the empirical dispersion correction was used. This was to be expected due to the fact that dispersion interactions are insufficiently described in most DFT functionals (including B3LYP).[25−27] There is also a previous study which showed that for the interaction of camphor with the same heme model, the equilibrium distance was shortened by a similar amount when using B3LYP-D compared to B3LYP.[28] Hence, one can expect that the structures produced by B3LYP-D3 are most likely more accurate than the B3LYP structures.

As was suggested by experimental studies,[4] we found the first step in the reaction mechanism to be a direct S oxidation, in which the iron-oxo oxygen binds to a lone pair belonging to the sulfur atom which is double bonded to the phosphorus atom. The oxygen−sulfur distance in the transition state (**TS^{Ox}**) was found to be significantly shorter for the quartet spin state compared to the doublet spin state (1.99 Å vs 2.22 Å for B3LYP and 2.00 Å vs 2.27 Å for B3LYP-D3). This indicates that the transition state is later for the quartet spin state than for the doublet spin state, which also is verified by the higher energy barrier in the quartet spin state (21 and 26 kJ/mol higher energy using B3LYP and B3LYP-D3, respectively, see Figure 5). The same effect of doublet versus quartet spin state on geometries and energies for the oxidation of heteroatoms

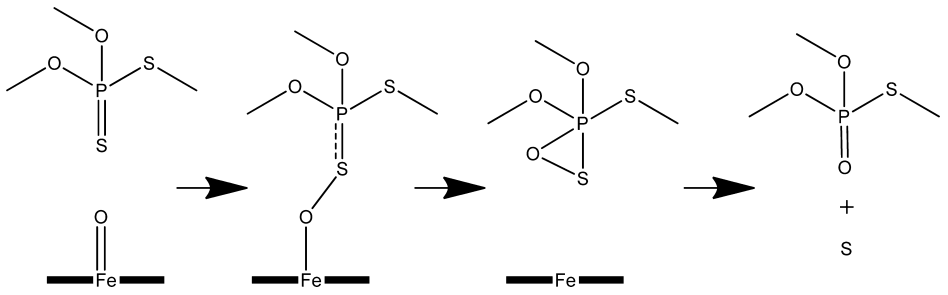

Figure 2. The previously suggested reaction mechanism. The Fe and bold lines represent the heme group.

dx.doi.org/10.1021/ct300347z | J. Chem. Theory Comput. XXXX, XXX, XXX−XXX

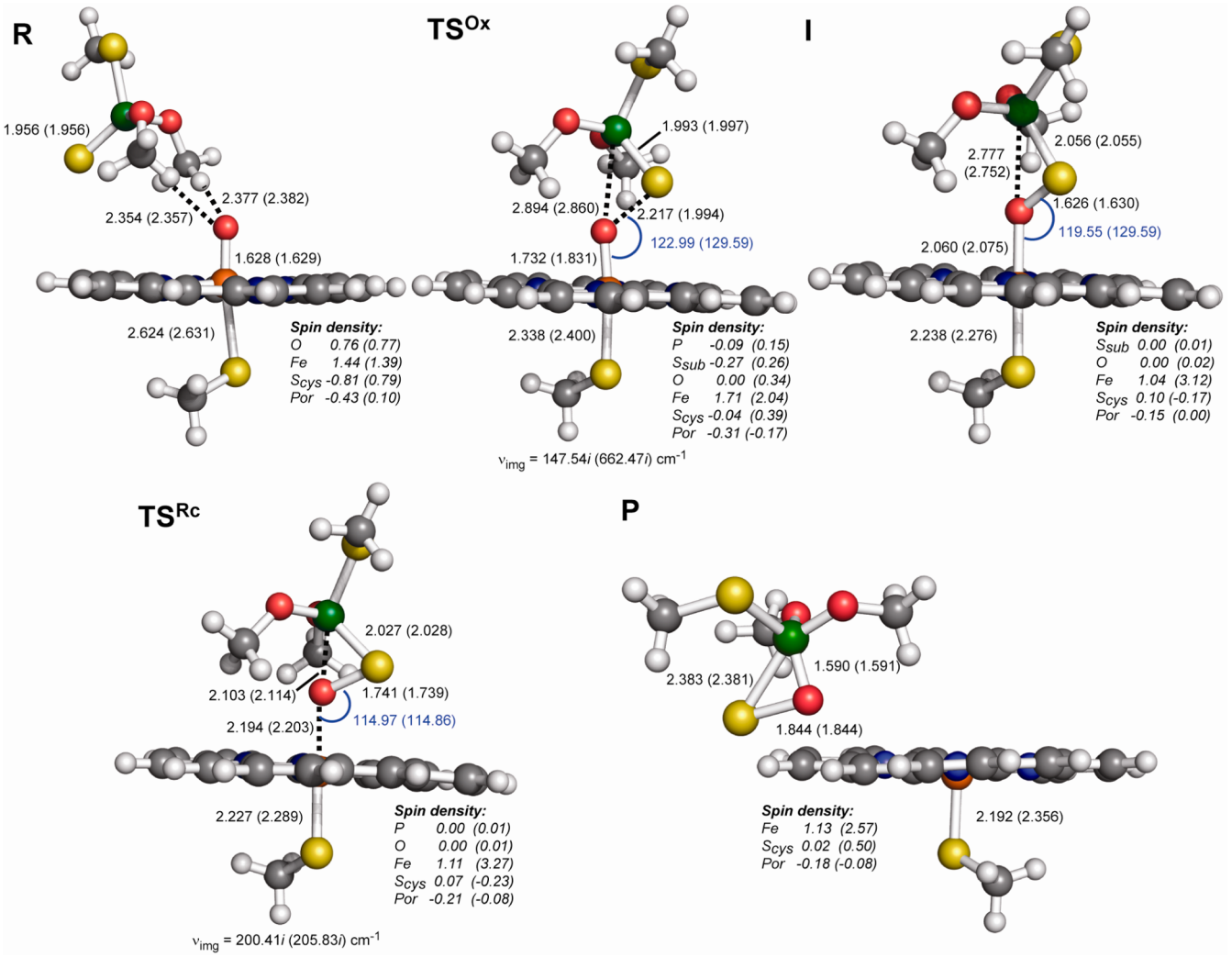

Figure 3. Structures, imaginary frequencies, geometrical features, and spin densities for the B3LYP calculations. All data are shown as doublet (quartet). Distances in Ångstroms are shown in black, and angles in degrees are shown in blue.

has previously been identified for the oxidation of thioethers,[29−31] sulfoxides,[29] and both tertiary[29,32] and primary amines.[33] Hence, the first step in the desulfurization can be considered as a standard CYP heteroatom oxidation, which most likely occurs in the doublet spin state. While the imaginary frequencies for the doublet spin state are quite small (148 and 62 cm^{-1} for B3LYP and B3LYP-D3, respectively), their normal modes do connect the reactants to the intermediates. Such small imaginary frequencies have been identified previously for sulfur oxidations by CYPs;[29,31] hence, they were not quite unexpected. Both the geometries and the spin densities for the reactant (**R**) and oxidation transition state (**TS^{Ox}**) are similar to the ones for the S-oxidation of the common thioether dimethylsulfide from a previous study.[29] The transition state is geometrically slightly later than the corresponding structure in dimethylsulfide oxidation, with a longer Fe−O bond and a shorter O−S bond.

In the sulfoxidized intermediate (**I**) the iron−oxygen bond is significantly elongated (0.4 Å compared to the reactant state), whereas only a slight elongation of the phosphor−sulfur bond occurs (0.1 Å). In the doublet spin state, this intermediate has a much lower energy than the reactant state (−36 kJ/mol for B3LYP and −45 kJ/mol B3LYP-D3), whereas in the quartet spin state, the intermediate energy is higher than that of the reactant state (16 kJ/mol for B3LYP and 10 kJ/mol for B3LYP-D3). The major difference between the B3LYP and B3LYP-D3 geometries for this intermediate is that the oxygen−phosphor distance is reduced by 0.2 Å when dispersion correction is included. This dispersion effect continues throughout the ring closure step, in which the energy barrier of the ring closure transition state (**TS^{Rc}**) relative to the intermediate (**I**) is much smaller for the B3LYP-D3 calculations (28 and 12 kJ/mol for B3LYP-D3 vs 48 and 44 kJ/mol for B3LYP, for the doublet and quartet spin states, respectively). Such a large energetic effect of including dispersion correction to a ring-opening/closing barrier has as far as we know not been observed previously. However, no such reaction barriers have been studied for triangular complexes. To determine if this is a general feature for ring closure to triangular complexes or a specific effect for this case in which a ring containing three heteroatoms is formed (among which, two are relatively large, phosphorus and sulfur), we investigated the previously studied ring closure step in the CYP mediated epoxidation of propene (the formation of the second C−O bond of the epoxide).[34] This barrier was in the previous study found to only exist in the quartet spin state; hence, we only investigated this spin state. The dispersion effects were found to be very small, only 2 kJ/mol, which also is similar to what was found for a ring-opening reaction of

dx.doi.org/10.1021/ct300347z | J. Chem. Theory Comput. XXXX, XXX, XXX−XXX

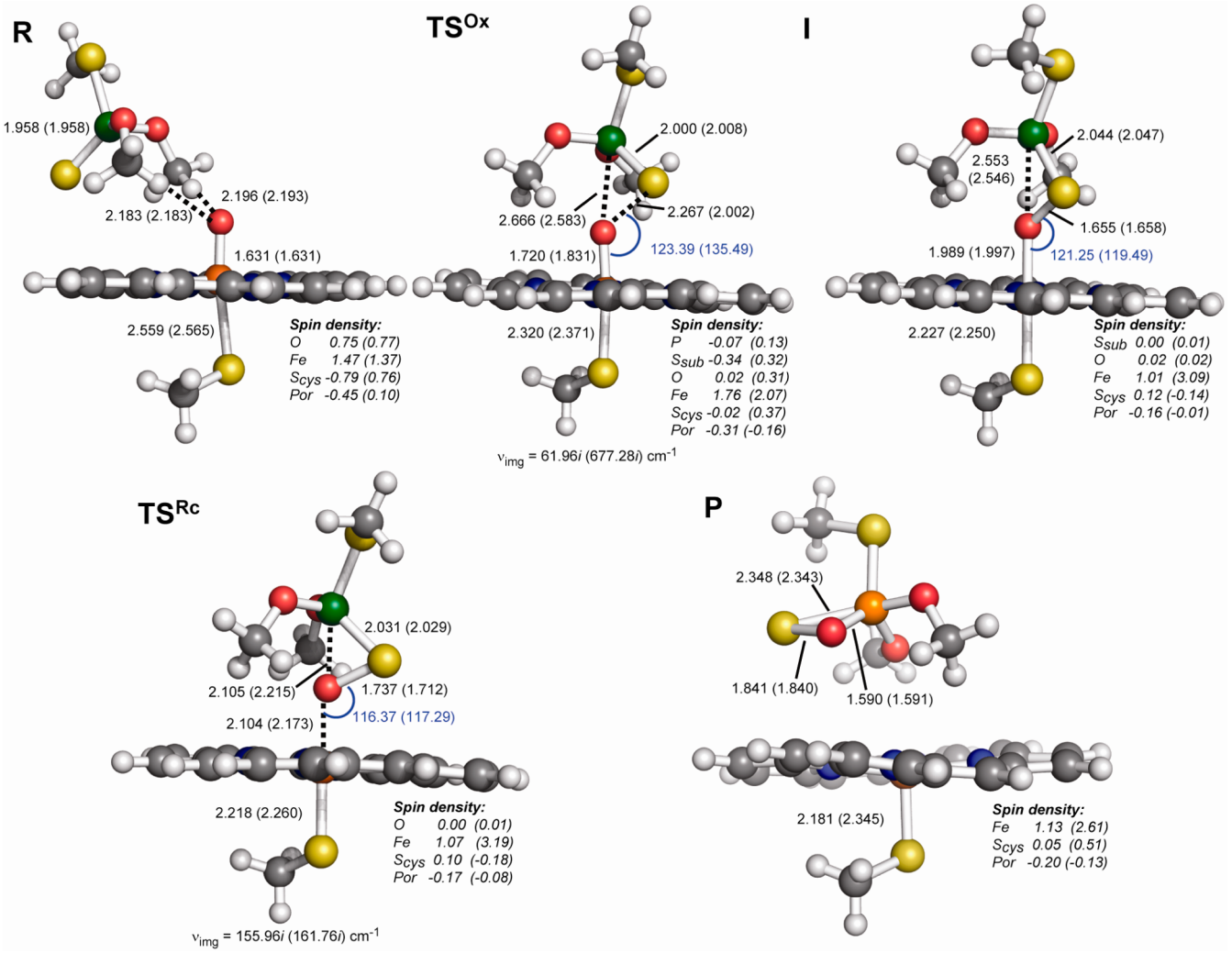

Figure 4. Structures, imaginary frequencies, geometrical features, and spin densities for the B3LYP-D3 calculations. All data are shown as doublet (quartet). Distances in Ångstroms are shown in black, and angles in degrees are shown in blue.

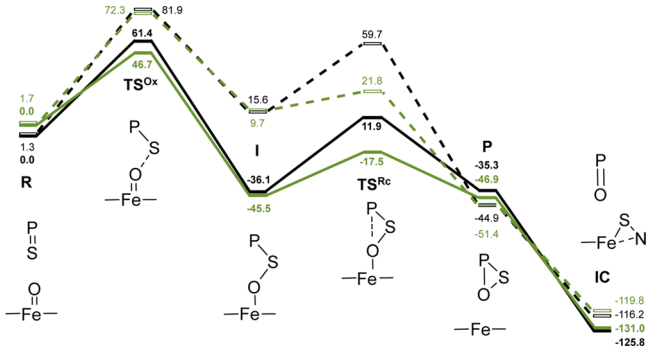

Figure 5. Energies in kJ/mol for the different states during the reaction mechanism calculated using B3LYP (black) and B3LYP-D3 (green). Doublet spin states are shown with solid lines, and quartet spin states are shown with dashed lines. Energies are from single-point calculations with the large basis set and include zero-point vibrational energies and solvent corrections computed with a dielectric constant of 4. Because oxidation barriers in CYPs computed without dispersion correction are better described relative to the separate compound I and substrate,[28] the B3LYP energies used to create the figure have been adjusted to give a better comparison to the B3LYP-D3 energies (however, the numbers shown are the actual energies).

oxanorbornene by Claeys et al. (which involved the opening of a C−O bond).[35] Hence, the large effect found here seems to at least not be general for either ring-opening/closure or triangular complexes. Thus, the dispersion effects of B3LYP-D3 on the formation of the triangular P−S−O oxathiirane complex seem to be unique among the ring-opening/closure reactions that have been studied so far, and it is hard to say if B3LYP or B3LYP-D3 is more accurate with regard to ring-closure reactions involving multiple heteroatoms. With regard to the structure of **TS^{Rc}**, it is quite interesting that the structures computed using B3LYP are similar in doublet and quartet spin states (Fe−O distance 2.2 Å and O−P distance 2.1 Å), whereas they are different when computed using B3LYP-D3 (Figures 3 and 4). The B3LYP-D3 **TS^{Rc}** in the doublet spin state has very similar Fe−O and O−P distances of 2.1 Å, whereas in the quartet spin state, both the distances are longer, ∼2.2 Å. In the last step, the formation of the phosphooxathiirane (**P**) from the ring closure transition state (**TS^{Rc}**), the product dissociates from the heme, and the O−P bond is shortened to 1.6 Å. From the point that the intermediate (**I**) has been formed, there is basically no spin density on either the substrate or the attached oxygen atom. Hence, the ring closure reaction is essentially a closed-shell reaction, since all of the spin density resides on the

dx.doi.org/10.1021/ct300347z | J. Chem. Theory Comput. XXXX, XXX, XXX−XXX

iron atom, the thiomethyl sulfur atom, and the porphyrin ring throughout this reaction.

To verify that there are no alternative reaction paths toward the formation of the phosphooxathiirane (**P**), we tried to locate a reaction path in which the iron-oxo oxygen attacked the phosphor−sulfur double bond directly. Attempts were made from multiple starting structures, and distance scans were performed with several reaction coordinates. However, all such attempts led to the location of the ring closure transition state ($\mathbf{TS^{Rc}}$), the normal modes of which led to the phosphooxathiirane (**P**) and the same intermediate that was found when investigating the direct S oxidation (**I**).

The inclusion of solvent effects (performed with the COSMO solvent model[21,36] using a dielectric constant of 4) gives higher reaction barriers for both transition states (see Figure 6), but the contribution is significantly larger for the ring

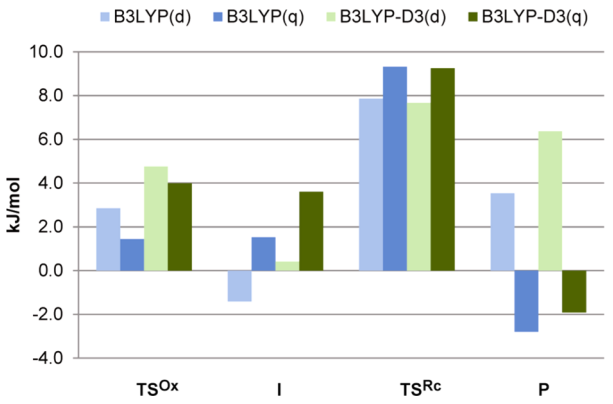

Figure 6. The effect of including solvent correction with an implicit solvent model with a dielectric constant of 4 relative to vacuum energies. The energies have been computed relative to the reactant state. B3LYP energies are shown in blue and B3LYP-D3 energies in green, with the doublet spin state in light color and the quartet spin state in dark color.

closure transition state compared to the oxidation transition state (on average 8.5 vs 3.3 kJ/mol). For the intermediate (**I**) and the phosphooxathiirane (**P**) complexes, the effects are in general smaller and vary between positive and negative. In general, it seems that the inclusion of solvent effects gives a more positive contribution to the energies when using B3LYP-D3 compared to B3LYP (see Figure 6). The only exception is the ring closure transition state ($\mathbf{TS^{Rc}}$), in which the solvent contribution is the same for both methods.

The phosphooxathiirane has been suggested to spontaneously lead to the formation of the final oxone, destruction or inactivation of heme, and the binding of sulfurs to cysteine residues in the protein.[5,37] Whether these reactions occur with the actual phosphooxathiirane or with atomic sulfur released from the phosphooxathiirane is still unknown.

Mechanistic Inhibition through Binding of Sulfur to the Heme Group. As suggested by Halpert et al.,[5] one possible reason for the apparent destruction of heme might be that the reactive sulfur atom formed when the phosphooxathiirane (**P**) is transformed into the final oxane product could bind directly to the heme iron atom, and possibly cause the iron atom to dissociate from the heme. To determine how a mechanistic inhibition could possibly occur, we investigated two likely mechanisms for the reaction of sulfur with heme. First, we studied the attack of the phosphooxathiirane sulfur atom on the heme iron atom, and second we studied the attack of the same sulfur on one of the nitrogen atoms bound to the heme iron atom. However, we found that both reaction paths lead to the same product, a triangular Fe−N−S complex (**IC**, see Figure 7), which gives rise to a highly distorted heme

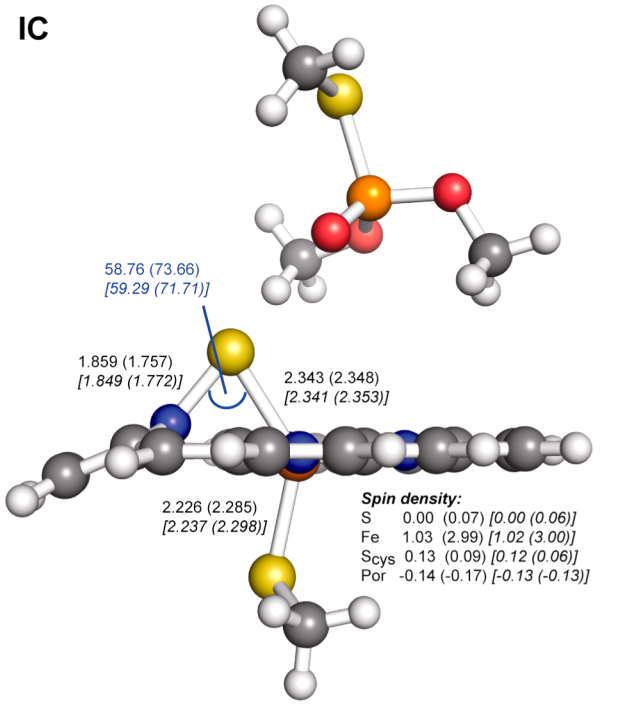

Figure 7. Structure, geometrical features, and spin densities from the B3LYP-D3 and B3LYP calculations of the inhibition complex. All data are shown as doublet D3 (quartet D3) *[doublet (quartet)]*, with B3LYP data in italic text. Distances in Ångstroms are shown in black, and angle in degrees are shown in blue.

structure in which the nitrogen atom is lifted out of the heme plane, causing its pyrrole ring to bend relative to the plane of the porphyrin ring, and the aromatic conjugation throughout the system is broken. The distortion is larger in the quartet spin state than in the doublet spin state, as can be seen by the Fe−S−N angle (see Figure 7). The formation of this complex was found to be barrierless when using both B3LYP and B3LYP-D3, and only a rotation of the oxathiirane intermediate (**P**) relative to the heme plane was required to initiate the formation of the inhibition complex. To verify that the triangular product was not a local minimum but the actual product, we also calculated the possible alternative product which would be formed through a pure Fe═S double bond (with a flat porphyrin ring). However, this product was found to be 17 kJ/mol higher in energy; thus the triangular complex is a more likely inhibition complex.

The formation of this triangular complex could be what creates the apparent destruction of heme, since the heme becomes distorted and the porphyrin ring is no longer a fully conjugated aromatic system. Hence, it is possible that this complex does not appear on UV spectra as a heme group. Also, the formation of this inhibition complex will interfere with the two most common ways to measure heme loss, measuring UV spectra of the pyridine hemochromogen and of the complex with carbon monoxide. Since both methods require binding of a ligand to the heme iron, which will cause a competition of binding of the ligand and the sulfur in the inhibition complex,

dx.doi.org/10.1021/ct300347z | J. Chem. Theory Comput. XXXX, XXX, XXX−XXX

the resulting measurements will be a result of the equilibrium between the inhibition complex and the ligand in question. The reason that Halpert et al.[5] could not explain the full loss of P450 could be that this equilibrium between inhibition complex and ligands used in measurements interfered with the summation of the total amount of P450 available.

To enable future experimental studies to directly investigate if this inhibition complex can be identified, we computed its UV spectra in the doublet spin state, shown in Figure 8 below

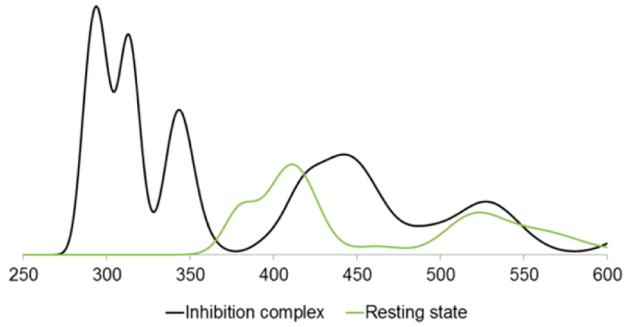

Figure 8. UV spectra of the inhibition complex and the Fe^{III} resting state computed using ZINDO/S.

together with the UV spectra of the Fe^{III} resting state computed with a bound water molecule. While the spectra are computed using the semiempirical ZINDO/S method, there are some peaks in the range 270−350 nm which only exist for the inhibition complex.

It has also been speculated that the nonexplained loss of heme could be due to the dissociation of iron from the heme moiety inside the enzyme active site;[5] however, no experimental evidence of this has been shown so far. The identified inhibition complex (**IC**) could potentially make it easier for iron to dissociate from the heme group, resulting in a porphyrin ring without iron which then would have completely different spectroscopic properties. The mechanism for the potential dissociation of iron from the heme in the inhibition complex is a subject that merits further studies.

CONCLUSIONS

The findings reported in this study support a previously suggested reaction mechanism for the desulfurization of phosphorodithioate pesticides by CYPs,[4] an initial sulfoxidation followed by a ring-closing and release of sulfur. The initial sulfoxidation step was found to have the highest energy barrier, behaving similarly to other sulfoxidations performed by CYPs.

While the inclusion of an empirical dispersion correction (B3LYP-D3) resulted in geometrical changes for most structures compared to nondispersion corrected calculations (B3LYP), it only showed significant energy differences for the ring-closing transition state, in which the inclusion of dispersion lowered the barrier relative to the preceding intermediate by 20 and 32 kJ/mol for the doublet and quartet spin states, respectively.

Finally, we located a new inhibition complex, with the sulfur atom of the pesticide binding to both the iron atom and a neighboring nitrogen atom in the porphyrin ring. This binding causes the pyrrole ring containing this nitrogen atom to bend out of the porphyrin plane, destroying part of the aromatic conjugation in the porphyrin ring. We suggest that this complex could be what creates the apparent destruction of heme that has been observed in experiments.

ASSOCIATED CONTENT

Supporting Information

Coordinates for all structures mentioned in the text. Tables with energies for all structures. This material is available free of charge via the Internet at http://pubs.acs.org.

AUTHOR INFORMATION

Corresponding Author

*Phone: (+45) 35 33 66 50. Fax: (+45) 35 30 60 41. E-mail: pry@farma.ku.dk.

Notes

The authors declare no competing financial interest.

ACKNOWLEDGMENTS

This work was supported by a grant from Lhasa Limited.

REFERENCES

(1) Heudorf, U.; Butte, W.; Schulz, C.; Angerer, J. . Reference values for metabolites of pyrethroid and organophosphorous insecticides in urine for human biomonitoring in environmental medicine. *Int. J. Hyg. Environ. Health* **2006**, *209*, 293−299.

(2) Sultatos, L. G. Mammalian toxicology of organophosphorus pesticides. *J. Toxicol. Environ. Health* **1994**, *43*, 271−289.

(3) Ptashne, K. A. Y. A.; Wolcott, R. M.; Neal, R. A. Oxygen-18 studies on the chemical mechanisms of the mixed function oxidase catalyzed desulfuration and dearylation reactions of Parathion. *J. Pharmacol. Exp. Ther.* **1971**, *179*, 380−385.

(4) Kamataki, T.; Lee Lin, M. C.; Belcher, D. H.; Neal, R. A. Studies of the metabolism of parathion with an apparently homogeneous preparation of rabbit liver cytochrome P-450. *Drug Metab. Dispos.* **1976**, *4*, 180−189.

(5) Halpert, J.; Hammond, D.; Neal, R. A. Inactivation of Purified Rat-Liver Cytochrome-P-450 During the Metabolism of Parathion (Diethyl Para-Nitrophenyl Phosphorothionate). *J. Biol. Chem.* **1980**, *255*, 1080−1089.

(6) Kamataki, T. E. T. S.; Neal, R. A. Metabolism of Diethyl p-Nitrophenyl Phosphorothionate (Parathion) by a Reconstituted Mixed-Function Oxidase Enzyme System: Studies of the Covalent Binding of the Sulfur Atom. *Mol. Pharmacol.* **1976**, *12*, 933−944.

(7) Ahlrichs, R.; Bar, M.; Haser, M.; Horn, H.; Kolmel, C. Electronic-Structure Calculations on Workstation Computers - the Program System Turbomole. *Chem. Phys. Lett.* **1989**, *162*, 165−169.

(8) Becke, A. D. Density-Functional Exchange-Energy Approximation with Correct Asymptotic-Behavior. *Phys. Rev. A* **1988**, *38*, 3098−3100.

(9) Lee, C. T.; Yang, W. T.; Parr, R. G. Development of the Colle-Salvetti Correlation-Energy Formula Into A Functional of the Electron-Density. *Phys. Rev. B* **1988**, *37*, 785−789.

(10) Becke, A. D. Density-Functional Thermochemistry. III. the Role of Exact Exchange. *J. Chem. Phys.* **1993**, *98*, 5648−5652.

(11) Vosko, S. H.; Wilk, L.; Nusair, M. Accurate Spin-Dependent Electron Liquid Correlation Energies for Local Spin-Density Calculations - A Critical Analysis. *Can. J. Phys.* **1980**, *58*, 1200−1211.

(12) Schafer, A.; Horn, H.; Ahlrichs, R. Fully Optimized Contracted Gaussian-Basis Sets for Atoms Li to Kr. *J. Chem. Phys.* **1992**, *97*, 2571−2577.

(13) Hehre, W. J.; Ditchfield, R.; Pople, J. A. Self-Consistent Molecular-Orbital Methods. XII. Further Extensions of Gaussian-Type Basis Sets for Use in Molecular-Orbital Studies of Organic-Molecules. *J. Chem. Phys.* **1972**, *56*, 2257−2261.

(14) Hariharan, P. C.; Pople, J. A. Influence of Polarization Functions on Molecular-Orbital Hydrogenation Energies. *Theor. Chim. Acta* **1973**, *28*, 213−222.

(15) Francl, M. M.; Pietro, W. J.; Hehre, W. J.; Binkley, J. S.; Gordon, M. S.; Defrees, D. J.; Pople, J. A. Self-Consistent Molecular-Orbital Methods. XXIII. A Polarization-Type Basis Set for Second-Row Elements. *J. Chem. Phys.* **1982**, *77*, 3654−3665.
(16) Krishnan, R.; Binkley, J. S.; Seeger, R.; Pople, J. A. Self-Consistent Molecular-Orbital Methods. XX. Basis Set for Correlated Wave-Functions. *J. Chem. Phys.* **1980**, *72*, 650−654.
(17) Mclean, A. D.; Chandler, G. S. Contracted Gaussian-Basis Sets for Molecular Calculations. I. Second Row Atoms, Z=11−18. *J. Chem. Phys.* **1980**, *72*, 5639−5648.
(18) Rulisek, L.; Jensen, K. P.; Lundgren, K.; Ryde, U. The reaction mechanism of iron and manganese superoxide dismutases studied by theoretical calculations. *J. Comput. Chem.* **2006**, *27*, 1398−1414.
(19) Mulliken, R. S. Electronic Population Analysis on LCAO-MO Molecular Wave Functions. I. *J. Chem. Phys.* **1955**, *23*, 1833.
(20) Grimme, S.; Antony, J.; Ehrlich, S.; Krieg, H. A consistent and accurate ab initio parametrization of density functional dispersion correction (DFT-D) for the 94 elements H-Pu. *J. Chem. Phys.* **2010**, 132.
(21) Klamt, A.; Schuurmann, G. Cosmo - A New Approach to Dielectric Screening in Solvents with Explicit Expressions for the Screening Energy and Its Gradient. *J. Chem. Soc., Perkin Trans. 2* **1993**, 799−805.
(22) Zerner, M. C.; Loew, G. H.; Kirchner, R. F.; Mueller-Westerhoff, U. T. An intermediate neglect of differential overlap technique for spectroscopy of transition-metal complexes. Ferrocene. *J. Am. Chem. Soc.* **1980**, *102*, 589−599.
(23) Anderson, W. P.; Edwards, W. D.; Zerner, M. C. Calculated spectra of hydrated ions of the first transition-metal series. *Inorg. Chem.* **1986**, *25*, 2728−2732.
(24) Neese, F. *ORCA − an ab Initio, Density Functional and Semiempirical Program Package*, version 2.6; University of Bonn: Bonn, Germany, 2008.
(25) Hobza, P.; Sponer, J.; Reschel, T. Density functional theory and molecular clusters. *J. Comput. Chem.* **1995**, *16*, 1315−1325.
(26) Allen, M. J.; Tozer, D. J. Helium dimer dispersion forces and correlation potentials in density functional theory. *J. Chem. Phys.* **2002**, *117*, 11113.
(27) Kristyán, S.; Pulay, P. Can (semi)local density functional theory account for the London dispersion forces? *Chem. Phys. Lett.* **1994**, *229*, 175−180.
(28) Lonsdale, R.; Harvey, J. N.; Mulholland, A. J. Inclusion of Dispersion Effects Significantly Improves Accuracy of Calculated Reaction Barriers for Cytochrome P450 Catalyzed Reactions. *J. Phys. Chem. Lett.* **2010**, *1*, 3232−3237.
(29) Rydberg, P.; Ryde, U.; Olsen, L. Sulfoxide, sulfur, and nitrogen oxidation and dealkylation by cytochrome P450. *J. Chem. Theory Comput.* **2008**, *4*, 1369−1377.
(30) Kumar, D.; Sastry, G. N.; de Visser, S. P. Effect of the Axial Ligand on Substrate Sulfoxidation Mediated by Iron(IV)-Oxo Porphyrin Cation Radical Oxidants. *Chem.—Eur. J.* **2011**, *17*, 6196−6205.
(31) Li, C.; Zhang, L.; Zhang, C.; Hirao, H.; Wu, W.; Shaik, S. Which Oxidant Is Really Responsible for Sulfur Oxidation by Cytochrome P450? *Angew. Chem., Int. Ed.* **2007**, *46*, 8168−8170.
(32) Li, C. S.; Wu, W.; Cho, K. B.; Shaik, S. Oxidation of Tertiary Amines by Cytochrome P450-Kinetic Isotope Effect as a Spin-State Reactivity Probe. *Chem.—Eur. J.* **2009**, *15*, 8492−8503.
(33) Rydberg, P.; Olsen, L. Do Two Different Reaction Mechanisms Contribute to the Hydroxylation of Primary Amines by Cytochrome P450? *J. Chem. Theory Comput.* **2011**, *7*, 3399−3404.
(34) de Visser, S. P.; Ogliaro, F.; Sharma, P. K.; Shaik, S. What factors affect the regioselectivity of oxidation by cytochrome P450? A DFT study of allylic hydroxylation and double bond epoxidation in a model reaction. *J. Am. Chem. Soc.* **2002**, *124*, 11809−11826.
(35) Claeys, D. D.; Stevens, C. V.; Roman, B. I.; Van De Caveye, P.; Waroquier, M.; Van Speybroeck, V. Experimental and computational study of the ring opening of tricyclic oxanorbornenes to polyhydro isoindole phosphonates. *Org. Biomol. Chem.* **2010**, *8*, 3644−54.
(36) Klamt, A.; Jonas, V.; Burger, T.; Lohrenz, J. C. W. Refinement and parametrization of COSMO-RS. *J. Phys. Chem. A* **1998**, *102*, 5074−5085.
(37) Kappers, W. A.; Edwards, R. J.; Murray, S.; Boobis, A. R. Diazinon is activated by CYP2C19 in human liver. *Toxicol. Appl. Pharmacol.* **2001**, *177*, 68−76.